Research Report: Evaluation of YOLOv12 for Multi-Modal Real-Time Visual UAV Detection

Julian Münzer
Student No. 294094

January 2026

Abstract

This study evaluates the performance of YOLOv12-nano for real-time UAV detection across Visible, Infrared, and Hybrid (interleaved) spectral modalities. Using the Anti-UAV300 dataset, we employed an experimental design consisting of 125 deterministic training runs per modality and validated results using non-parametric statistical tests. Results demonstrate that Visible and Infrared modalities achieve equivalent performance (mAP50 $\approx 96.7\%$), confirming thermal imagery as a robust alternative to visible light. Conversely, the Hybrid data-level fusion strategy showed a reduction in localization accuracy (mAP50-95). While the omnibus Friedman test indicated a significant main effect with a large effect size ($\eta^2 = 0.173$), specific pairwise differences did not survive conservative Hommel correction. We conclude that while single-modality detection is highly effective, naive spectral mixing hinders convergence in single-backbone architectures, suggesting the need for specialized fusion mechanisms. Code available at `https://github.com/julsmzr/uav-ai`.

1 Research

1.1 Research Plan

The primary goal of this research is the comparative analysis of YOLOv12 [6] performance across visible light, infrared spectrum, and Hybrid modalities for real-time UAV detection. This study evaluates the multi-modal data-level fusion approach ('Hybrid') against single-modality systems.

The research objectives are to quantify detection performance across spectral modalities and validate differences using statistical analysis. This includes a comparison of Precision, Recall, and Mean Average Precision alongside non-parametric statistical tests to ensure robust validation.

Premises and Assumptions:

- Infrared modality provides complementary information to visible light.
- A Hybrid approach may leverage advantages of both spectral domains.
- Repeated stratified k-fold cross-validation ensures robust estimation.
- YOLOv12-nano [6] represents state-of-the-art real-time detection capabilities.

1.2 Datasets

To validate the proposed multi-modal objectives, we selected a benchmark providing high-fidelity, synchronized visual and infrared-spectral streams to ensure fair comparison.

1.2.1 Anti-UAV300 Dataset

The Anti-UAV300 dataset [4], contains 318 video sequences with two synchronized streams: Visible and Infrared. The dataset comprises 593,802 combined frames featuring real-valued pixel intensities, designed specifically for UAV detection and tracking research.

Spectrum	Total Frames	Annotated Frames	Coverage
Visible	296,901	280,218	94.38%
Infrared	296,901	293,209	98.76%
Total	**593,802**	**573,427**	**96.57%**

Table 1: AntiUAV-300 Dataset composition and annotation rates per modality [4]

1.2.2 Dataset Pre-processing and Stratification

To ensure efficient experimentation while maintaining statistical robustness, the dataset was processed using a stratified subsampling strategy:

- **Format Conversion:** Source MP4 streams were extracted into individual JPEG frames.
- **Label Cleaning:** Annotations were parsed from the source JSON files and converted to normalized COCO format $(x_{\text{center}}, y_{\text{center}}, w, h)$.
- **Stratified Subsampling:** A shuffled subset of $N = 1{,}000$ frames was sampled from the visible spectrum using a cryptographically secure random seed. The sampling maintained the original class balance, resulting in 56 background frames and 944 annotated frames (approximately 1:17 ratio).

1.3 Research Environment

Experiments were executed on macOS (Apple Silicon M4 Chip with 10 CPU Cores and 10 GPU Cores) using Metal Performance Shaders (MPS). The software stack included Python 3.13.5 with PyTorch, scikit-learn, pandas, numpy, scipy, pingouin for machine learning and statistical analysis; Ultralytics YOLOv12 [6] for object detection; and R 4.5.2 for independent statistical verification.

2 Statistical Methodology and Measures

2.1 Performance Measures

Precision (P) and Recall (R) measure the trade-off between false positives and false negatives:

$$P = \frac{TP}{TP + FP}, \quad R = \frac{TP}{TP + FN} \tag{1}$$

Mean Average Precision (mAP) is defined as the mean of the Average Precision across all classes and/or IoU thresholds. AP is calculated as the area under the Precision-Recall curve:

$$AP = \int_0^1 p(r)\, dr \tag{2}$$

where $p(r)$ is the precision at recall r. We report mAP50 (IoU threshold of 0.50) and mAP50-95 (averaged across IoU thresholds from 0.50 to 0.95 in steps of 0.05), with the latter providing a more strict measure of localization accuracy.

2.2 Non-Parametric Statistical Testing

Non-parametric tests are appropriate when the assumption of normally distributed data cannot be guaranteed, which is common when comparing machine learning algorithms across multiple folds or datasets. Following the recommendations of Demšar (2006) [2], we employ the Friedman test for omnibus comparison and the Wilcoxon signed-rank test with Hommel correction for pairwise analysis.

2.2.1 Friedman Test

The Friedman test is a non-parametric alternative to repeated-measures ANOVA. We describe the calculation method used by the R `stats` package to illustrate the test statistic. It ranks the performance of k algorithms across n experimental runs.

$$\chi_F^2 = \frac{12\sum_{j=1}^{k}(R_j - \bar{R})^2}{nk(k+1) - \frac{1}{k-1}\sum_{i=1}^{n}\sum_{g=1}^{g_i}(t_{i,g}^3 - t_{i,g})} \tag{3}$$

where $R_j = \sum_{i=1}^{n} r_i^j$ is the sum of ranks for the j-th algorithm, and $\bar{R} = n(k+1)/2$ is the expected sum of ranks. The denominator includes a correction for ties, where $t_{i,g}$ is the number of ties in the g-th group of ties within the i-th fold. If no ties are present, the term vanishes, simplifying to the standard formula. Under the null hypothesis, this statistic follows a chi-squared distribution with $k-1$ degrees of freedom.

The p-value is computed using the cumulative distribution function of the chi-squared distribution:

$$p = P(\chi_{k-1}^2 \geq \chi_F^2) \tag{4}$$

This corresponds to the area under the upper tail of the chi-squared density curve with $k-1$ degrees of freedom.

2.2.2 Pairwise Wilcoxon Signed-Rank Test

Post-hoc pairwise comparisons are conducted using the Wilcoxon signed-rank test. We present the specific algorithm used by the R `stats` package to calculate the statistic.

First, differences between the two algorithms are calculated for each fold, and differences equal to zero are discarded, reducing the sample size to n'. The absolute differences are ranked, and the test statistic V is the sum of ranks corresponding to positive differences. To strictly match the R implementation, we compute the z-statistic using the normal approximation with a continuity correction and a correction for ties:

$$z = \frac{|V - \frac{n'(n'+1)}{4}| - 0.5}{\sqrt{\frac{n'(n'+1)(2n'+1)}{24} - \frac{1}{48}\sum_g(t_g^3 - t_g)}} \tag{5}$$

where n' is the number of non-zero differences, and t_g is the number of ties in the g-th group of tied ranks. The term 0.5 is the continuity correction. The p-value for the two-sided test is calculated from the standard normal distribution: $p = 2 \times P(Z \geq |z|)$.

2.2.3 Hommel's Correction Procedure

To control the Family-Wise Error Rate (FWER) across the $m = \frac{k(k-1)}{2}$ pairwise comparisons, we apply Hommel's procedure as implemented in the R `p.adjust` function.

R calculates adjusted p-values (p_{adj}) such that a hypothesis is rejected at level α if $p_{adj} \leq \alpha$. The procedure is defined as follows: let $p_{(1)} \leq p_{(2)} \leq \cdots \leq p_{(m)}$ be the ordered raw p-values. We find the largest integer $j \in \{1, \ldots, m\}$ satisfying:

$$p_{(m-j+q)} > \frac{q\alpha}{j} \quad \text{for all } q = 1, \ldots, j \tag{6}$$

If no such j exists, all hypotheses are rejected. Otherwise, we reject all hypotheses H_i with raw p-values $p_i \leq \frac{\alpha}{j}$.

2.3 Effect Size: Eta Squared (η^2)

We utilize η^2 to measure the proportion of variance explained by the modality factor::

$$\eta^2 = \frac{SS_{\text{effect}}}{SS_{\text{total}}} \tag{7}$$

where the Sum of Squares components are calculated on the ranks:

$$SS_{\text{effect}} = n \sum_{j=1}^{k} (\bar{r}_{\cdot j} - \bar{r}_{\cdot\cdot})^2 \tag{8}$$

$$SS_{\text{total}} = \sum_{i=1}^{n} \sum_{j=1}^{k} (r_{ij} - \bar{r}_{\cdot\cdot})^2 \tag{9}$$

Notation: n: number of folds; k: number of modalities; r_{ij}: rank of fold i and modality j; $\bar{r}_{\cdot j}$: mean rank of modality j; $\bar{r}_{\cdot\cdot}$: grand mean rank ($(k+1)/2$).

Following Cohen's conventions for the effect size index f [1], we derive the corresponding η^2 thresholds using the relation $\eta^2 = f^2/(1+f^2)$. Consequently, values of 0.01, 0.06, and 0.14 are considered small, medium, and large effect sizes, respectively.

3 Multi-Modal UAV Detection Experiments

3.1 General Experimental Design

All experiments share a synchronized architecture to ensure validity and reproducibility. Deterministic behavior was enforced through cryptographically secure seed generation: seven seeds were generated using Python's `secrets` module and hashed through MD5 to produce 32-bit integer seeds. One seed controlled the stratified subsampling, one the cross-validation folding, and five seeds initialized distinct model weight configurations.

The experimental pipeline (visual graph in Appendix A) consisted of: (1) data ingestion and preprocessing, (2) stratified k-fold partitioning, (3) model training with deterministic initialization, and (4) multi-implementation statistical analysis.

The shared configuration across all experiments was:

- **Model:** YOLOv12-nano, pre-trained on COCO [6]
- **Input Resolution:** 640 pixels (images resized preserving aspect ratio)
- **Validation:** Repeated Stratified K-Fold with 5 splits and 5 repeats ($5 \times 5 = 25$ folds per seed)
- **Weight Initialization:** 5 distinct seeds, yielding $25 \times 5 = 125$ training runs per modality
- **Training:** 20 epochs per fold, AdamW optimizer with learning rate 0.01, batch size 16
- **Augmentation:** Standard YOLO augmentations including mosaic, random flip, and HSV adjustments

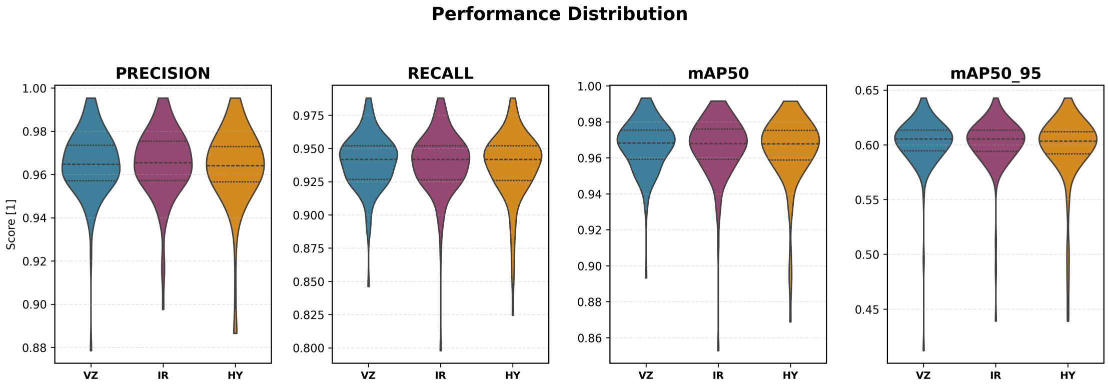

Modality	Precision	Recall	mAP50	mAP50-95
Visible (VZ)	0.9653 ± 0.0057	0.9401 ± 0.0060	0.9669 ± 0.0039	0.6020 ± 0.0095
Infrared (IR)	0.9653 ± 0.0054	0.9394 ± 0.0066	0.9662 ± 0.0059	0.6015 ± 0.0096
Hybrid (HY)	0.9632 ± 0.0063	0.9369 ± 0.0078	0.9644 ± 0.0058	0.5960 ± 0.0111

Table 2: Distribution and summary statistics of detection performance. The violin plots visualize the kernel density estimation across 25 data blocks, highlighting the stability of results for Visible (VZ), Infrared (IR), and Hybrid (HY) modalities. The table below details the corresponding quantitative metrics (Mean ± Std).

Final metrics were computed by averaging across the 5 folds for each of the seeded repetitions, producing 25 aggregated samples per modality for statistical analysis.

3.2 Experiment 1: Visible Light (VZ)

Input Data: Standard RGB camera imagery extracted from the visible stream of the Anti-UAV300 dataset. Images have a native resolution of 1920 × 1080 pixels, resized to 640 × 360 during training.

Goal: Establish baseline detection performance under standard lighting conditions.

3.3 Experiment 2: Infrared (IR)

Input Data: Thermal infrared imagery synchronized to the visible subset frames. Images have a native resolution of 640 × 512 pixels.

Goal: Evaluate detection capabilities in the thermal spectrum, which captures heat signatures independent of ambient lighting.

3.4 Experiment 3: Hybrid (HY)

Input Data: An interleaved dataset comprising the first 50% of visible frames and the second 50% of infrared frames within the same training batches.

Goal: Assess whether early-fusion multi-modal training improves generalization by exposing the model to both spectral domains simultaneously.

Implementation	**Friedman**	**Wilcoxon**	**Hommel**
SciPy	✓	✓	–
R	✓	✓	✓
Pingouin	✓	✓	–
STAC	✓	–	–
Statsmodels	–	–	✓

Table 3: Statistical Test Implementation Coverage

4 Statistical Analysis Results

To guarantee reliability and guard against implementation-specific artifacts such as value approximations, results were cross-verified across five independent statistical implementations: SciPy and Pingouin in Python, R's native statistical functions, STAC (Statistical Tests for Algorithms Comparison) [5], and Statsmodels for Hommel correction. Not all implementations support all tests; Table 3 summarizes coverage.

4.1 Friedman Test Results

The Friedman test was applied to determine whether significant differences exist among the three modalities. Results were consistent across implementations (Table 4).

The Friedman test revealed a significant difference among modalities only for mAP50-95 ($p = 0.013$, significant at $\alpha = 0.05$). Precision, Recall, and mAP50 showed no significant omnibus differences, indicating that modality choice does not meaningfully affect these metrics.

4.2 Pairwise Wilcoxon Tests with Hommel Correction

For mAP50-95, where the Friedman test indicated significance, pairwise Wilcoxon signed-rank tests were conducted between all modality pairs: VZ vs IR, IR vs HY, and VZ vs HY. Raw p-values were corrected using Hommel's procedure.

While the Friedman test indicated an overall effect of modality on mAP50-95, subsequent Hommel-corrected pairwise comparisons did not identify specific significant pairs. The IR vs HY and VZ vs HY comparisons approached significance (uncorrected $p \approx 0.06$), but corrections for multiple testing rendered these non-significant. This suggests that the Hybrid modality may introduce subtle degradation in localization accuracy, but the effect is not strong enough to survive correction.

4.3 Effect Size Analysis

Effect sizes (η^2) quantify the practical magnitude of modality effects independent of sample size (Table 6).

Metric	**SciPy**	**R**	**Pingouin**	**STAC**
Precision	0.203	0.203	0.206	0.411
Recall	0.071	0.071	0.070	0.224
mAP50	0.057	0.057	0.057	0.198
mAP50-95	**0.013***	**0.013***	**0.011***	0.082

Table 4: Friedman Test Results Across Implementations

*Significant at $\alpha = 0.05$. STAC uses the Iman-Davenport correction [3] with an F-distribution, whereas SciPy, R, and Pingouin use the standard chi-squared approximation. We report both approaches; however, because our sample size (n=25) is sufficiently large for the chi-squared approximation to be accurate, we base our primary conclusions on the results from SciPy, R, and Pingouin.

Implementation	VZ vs IR	IR vs HY	VZ vs HY
SciPy + Statsmodels	1.000 / 1.000	0.058 / 0.116	0.065 / 0.131
R	0.953 / 0.953	0.056 / 0.111	0.063 / 0.125
Pingouin	1.000 / 1.000	0.060 / 0.119	0.066 / 0.133

Table 5: Pairwise Wilcoxon P-Values for mAP50-95 (Raw / Hommel-Corrected)

No pairwise comparison reached significance at $\alpha = 0.05$ after Hommel correction.

The effect size for mAP50-95 ($\eta^2 = 0.173$) exceeds Cohen's threshold of 0.14 for a large effect, indicating that modality explains a substantial proportion of variance in localization accuracy. This aligns with the significant Friedman result and suggests that while all modalities achieve similar detection rates, precision of bounding box localization varies meaningfully across spectral inputs.

4.4 Limitations

Using 1,000 frames (≈0.17% of the full dataset) may limit generalizability despite stratified sampling. Second, our Hybrid approach constitutes data-level fusion rather than true multi-modal fusion with dedicated feature extractors; conclusions about multi-modal detection should not be extrapolated to architectures with late-fusion or attention mechanisms. Third, the 25 statistical samples per modality derive from averaged fold metrics within shared cross-validation partitions, introducing partial dependency that may affect test assumptions. Finally, results are specific to YOLOv12-nano and the Anti-UAV300 benchmark.

5 Summary of Research

This study evaluated YOLOv12-nano performance across three spectral modalities for UAV detection using an experimental design with 125 training runs per modality and multi-implementation statistical validation.

Modality Equivalence: Visible and Infrared modalities achieved statistically equivalent performance across Precision (96.53%), Recall (≈94%), and mAP50 (≈96.7%). This confirms that uncalibrated thermal imagery is as effective as RGB for UAV detection in this benchmark, validating infrared as a viable alternative for conditions where visible light is insufficient.

Hybrid Performance: The interleaved Hybrid approach resulted in slight degradation, particularly in localization accuracy (mAP50-95: 59.60% vs 60.20% for VZ). The Friedman test detected a significant overall modality effect on mAP50-95 ($p = 0.013$) with a large effect size ($\eta^2 = 0.173$). However, pairwise comparisons did not survive Hommel correction, suggesting the degradation is subtle. This performance drop likely stems from conflicting feature distributions between the visible and infrared spectra, which hinders convergence when optimizing a single shared backbone without modality-specific feature extractors.

Conclusion: For the Anti-UAV300 benchmark using YOLOv12, single-modality systems (either Visible or Infrared) are sufficient and may even be preferable to naive multi-modal fusion. Future work should explore late-fusion or attention-based multi-modal architectures that can better leverage complementary spectral information.

Metric	η^2	Interpretation
Precision	0.064	Medium
Recall	0.106	Medium
mAP50	0.114	Medium
mAP50-95	0.173	Large

Table 6: Effect Sizes (η^2) by Metric

References

[1] J. Cohen. *Statistical Power Analysis for the Behavioral Sciences.* Lawrence Erlbaum Associates, 1988.

[2] Janez Demšar. Statistical comparisons of classifiers over multiple data sets. *Journal of Machine Learning Research*, 7:1–30, 2006.

[3] Ronald L. Iman and James M. Davenport. Approximations of the critical region of the Friedman statistic. *Communications in Statistics - Theory and Methods*, 9(6):571–595, 1980.

[4] Nan Jiang, Kuiran Wang, Xiaoke Peng, Xuehui Yu, Qiang Wang, Junliang Xing, Guorong Li, Jian Zhao, Guodong Guo, and Zhenjun Han. Anti-uav: A large multi-modal benchmark for uav tracking, 2021.

[5] Ismael Rodríguez-Fdez, Adrián Canosa, Manuel Mucientes, and Alberto Bugarín. STAC: a web platform for the comparison of algorithms using statistical tests. In *Proceedings of the 2015 IEEE International Conference on Fuzzy Systems (FUZZ-IEEE)*, 2015.

[6] Yunjie Tian, Qixiang Ye, and David Doermann. Yolo12: Attention-centric real-time object detectors. *arXiv preprint arXiv:2502.12524*, 2025.

A Experiment Pipeline

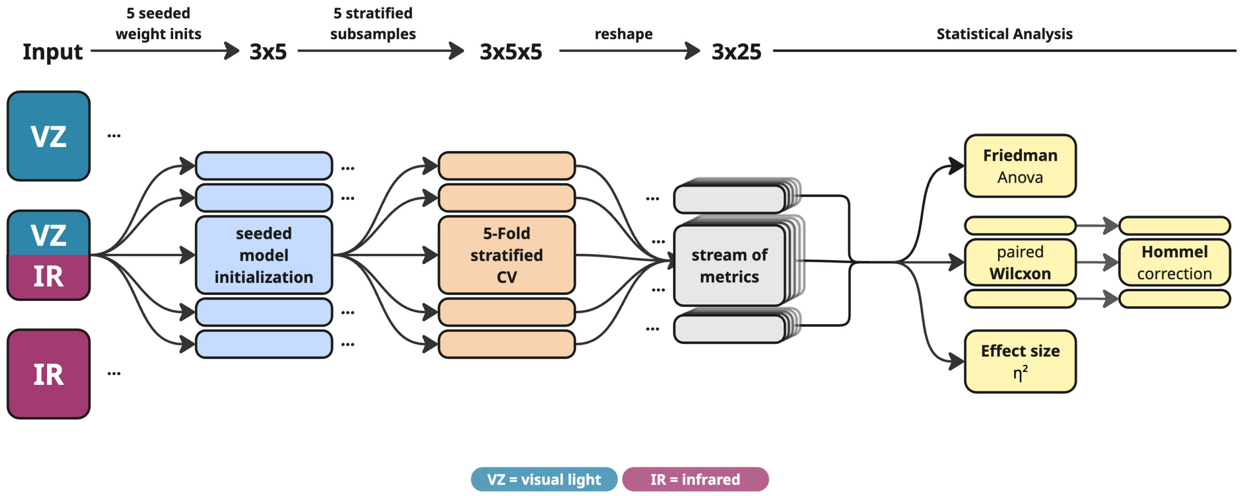

Figure 1: Experiment Pipeline